J. Fluid Mech. (2015), *vol.* 770, R2, doi:10.1017/jfm.2015.148

JFM RAPIDS
journals.cambridge.org/rapids

On the anisotropic response of a Janus drop in a shearing viscous fluid

Misael Díaz-Maldonado[1] **and Ubaldo M. Córdova-Figueroa**[1,†]

[1]Department of Chemical Engineering, University of Puerto Rico – Mayagüez, Mayagüez, PR 00681, USA

(Received 1 December 2014; revised 24 January 2015; accepted 4 March 2015; first published online 27 March 2015)

The force and couple that result from the shearing motion of a viscous, unbounded fluid on a Janus drop are the subjects of this investigation. A pair of immiscible, viscous fluids comprise the Janus drop and render it with a 'perfect' shape: spherical with a flat, internal interface, in which each constituent fluid is bounded by a hemispherical domain of equal radius. The effect of the arrangement of the internal interface (drop orientation) relative to the unidirectional shear flow is explored within the Stokes regime. Projection of the external flow into a reference frame centred on the drop simplifies the analysis to three cases: (i) a shear flow with a velocity gradient parallel to the internal interface, (ii) a hyperbolic flow, and (iii) two shear flows with a velocity gradient normal to the internal interface. Depending on the viscosity of the internal fluids, the Janus drop behaves as a simple fluid drop or as a solid body with broken fore and aft symmetry. The resultant couple arises from both the straining and swirling motions of the external flow in analogy with bodies of revolution. Owing to the anisotropic resistance of the Janus drop, it is inferred that the drop can migrate lateral to the streamlines of the undisturbed shear flow. The grand resistance matrix and Bretherton constant are reported for a Janus drop with similar internal viscosities.

Key words: drops and bubbles, low-Reynolds-number flows, multiphase flow

1. Introduction

Compound multiphase drops arise in diverse processes of engineering interest such as direct-contact heat exchangers, melting of ice particles falling in the atmosphere, rapid evaporation of liquids at superheated conditions, explosions of multicomponent fuel drops, and in several other settings (Johnson & Sadhal 1985). Typically, a pair of fluid phases immersed in a host fluid constitute the compound multiphase drop,

† Email address for correspondence: ubaldom.cordova@upr.edu

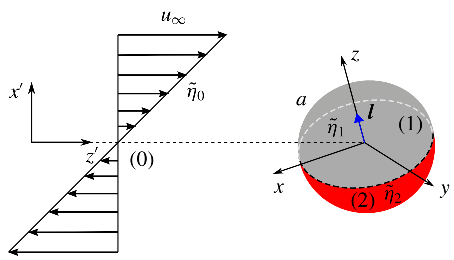

FIGURE 1. A 'perfect' Janus drop subject to a unidirectional shear flow. The vector $\boldsymbol{l}$ is parallel to the axis of symmetry of the Janus drop and points towards the less viscous fluid.

where one of the phases may engulf completely or partially its counterpart (Torza & Mason 1970). A limiting configuration of actual interest for the fabrication of anisotropic particles arises when two drops (of similar interfacial tension) undergo partial engulfment, leading to the formation of a compound drop of nearly spherical shape and an almost flat, internal interface (Guzowski *et al.* 2012). This particular object is usually referred to as a Janus drop – named after the Roman god. The Janus drop is considered to be 'perfect' when the constituent fluid phases are each bounded by a hemispherical domain of equal radius, or equivalently when the drop exhibits a flat, internal interface (Shklyaev *et al.* 2013), where the latter is referred to as 'the internal interface' from this point onward for brevity.

This study aims to characterise the hydrodynamic response (forces and couples) of a 'perfect' Janus drop subject to the shearing motion of a viscous unbounded fluid (ubiquitous flow type), and considers how this response is affected by the drop orientation (a factor absent in single-phase drops). A schematic representation of a Janus drop of arbitrary orientation in a simple shear flow is provided in figure 1. The orientation of the Janus drop is defined by the unit vector $\boldsymbol{l}$, which is normal to the internal interface. This study reveals that the anisotropic properties of the Janus drop arise from the presence of the internal interface; the viscosity of the constituent fluids is of secondary importance.

Previous theoretical studies have considered the dynamics of compound multiphase drops in streaming axisymmetric flows (Rushton & Davies 1983; Sadhal & Oguz 1985) and in Marangoni-driven flows (Morton, Subramanian & Balasubramaniam 1990; Rosenfeld, Lavrenteva & Nir 2009). Fluid motion is usually analysed in the limit of non-deformable interfaces, with the exception of the contributions of Chervenivanova & Zapryanov (1989) and Vuong & Sadhal (1989). The latter study reveals little dependence of the drag force on the shape distortion, which justifies the neglect of interface deformations in prior studies. Stone & Leal (1990) studied the deformation and breakup of concentric drops in linear flows. Recently, Shardt, Derksen & Mitra (2014) studied the dynamics of a Janus drop in a simple shear flow; however, within the restriction of a two-dimensional (2D) flow everywhere.

It is intriguing to note that cross-flow migration of compound multiphase drops appears to be a fairly unexplored problem despite important implications in mixing phenomena. For instance, lateral migration can induce coalescence of initially unaligned drops (Manga & Stone 1993). Interestingly, a Janus drop can display cross-flow migration in a streaming flow because of the anisotropic resistance imparted by the internal interface (Shklyaev *et al.* 2013). From the perspective of hydrodynamic resistances, the Janus drop behaves as a body of revolution (e.g. spheroid), such that the drag force is generally not parallel to the flow. The key finding is that cross-flow migration can occur without the influence of interface deformations associated with wall interactions or non-uniform velocity gradients, which are needed to induce the migration of single-phase drops.

The outline of the article is presented here. The problem statement is formulated in § 2, where for an arbitrary drop orientation the external shear flow is broken down into flows with velocity gradients normal and parallel to the internal interface. The equations that govern fluid motion are presented in § 3, and solved in the creeping motion limit in § 4. The influence of the viscosity of the three fluid phases is incorporated into the analysis for completeness. In § 4.1, it is shown that the Janus drop behaves as a single-phase drop under the action of a shear flow with a velocity gradient parallel to the internal interface. The force imposed on the Janus drop by a plane hyperbolic flow is analysed in § 4.2. It is found that the equilibrium orientation of the Janus drop in a hyperbolic flow occurs when the internal interface is aligned with the axis of strain or compression. The Janus drop is expected to respond with a couple that restores this particular arrangement under an external perturbation. In § 4.3, the force and couple imposed by a shear flow with a velocity gradient normal to the internal interface of the Janus drop are studied. It is found that the resultant couple arises from both the straining and rotating components of the shear flow, similar to bodies of revolution. From a practical point of view, knowledge of the behaviour of a Janus drop in a shear flow is a first step in understanding its dynamics in experiments (e.g. Poiseuille flows or microfluidic settings). Along this line of thought, the migration velocity of a Janus drop lateral to a streaming flow is presented in § 4.4. Concluding remarks are given in § 5, where the conditions for the occurrence of the cross-flow migration of a Janus drop in a shear flow are briefly discussed. In the appendix, the grand resistance matrix and Bretherton (1962) constant are provided on account of their potential relevance to experimenters. Since Janus drops typically comprise fluids of similar viscosity in microfluidic settings (Nisisako *et al.* 2006), the results of the appendix are narrowed down to this limit of practical interest. Interestingly, the coupling tensor, which characterises the torque on a body in a streaming flow and the force in a rotational flow, is found to be identically zero at the centre of hydrodynamic reaction of the Janus drop. Additionally, it is found that the shear force vanishes at the centre of reaction and, therefore, the dynamics of a 'freely' suspended Janus drop in a shear flow are identical to that of a spheroid of revolution (Jeffery 1922). The stresslet of a Janus drop in an elongational flow (axisymmetric) is identical to the stresslet produced by a single-phase drop. For transversal straining flows, the stresslet is found to be intermediate to that of a single-phase drop and a solid sphere.

2. Problem statement

Figure 1 depicts a neutrally buoyant Janus drop immersed in a viscous shearing fluid, which is denoted by '0'. The Janus drop comprises two internal fluids, denoted by '1' and '2'. The dynamic viscosity of each fluid phase ($j=0,1,2$) is defined by $\tilde{\eta}_j$; conventionally, it is assumed that $\tilde{\eta}_1 \leqslant \tilde{\eta}_2$. The principal objective of this investigation is to calculate the force and couple on a Janus drop centred in a simple shear flow with zero mean velocity:

$$\boldsymbol{u}_\infty = \tfrac{1}{2} G\left(\boldsymbol{E}^\infty \boldsymbol{\cdot} \boldsymbol{x}' + \boldsymbol{e}'_z \times \boldsymbol{x}'\right) = G x' \boldsymbol{e}'_z, \tag{2.1}$$

where G is a constant shear rate, $\boldsymbol{E}^\infty$ is the rate-of-strain tensor of the undisturbed flow, and $\boldsymbol{x}' = (x', y', z')$ is a set of space-fixed Cartesian coordinates, with corresponding unit vectors ($\boldsymbol{e}'_x$, $\boldsymbol{e}'_y$, $\boldsymbol{e}'_z$), that ensure a unidirectional flow. The drop orientation effect is considered by projecting $\boldsymbol{u}_\infty$ into a reference frame centred and affixed to the Janus drop $\boldsymbol{x} = (x, y, z)$ via the transformation $\boldsymbol{x}' = \boldsymbol{A}\boldsymbol{x}$, where the transformation matrix $\boldsymbol{A}$ parametrises the drop orientation from a coincident arrangement of both sets of axes:

$$\boldsymbol{A} = \begin{pmatrix} \cos\alpha & 0 & -\sin\alpha \\ -\sin\alpha\sin\beta & \cos\beta & -\cos\alpha\sin\beta \\ \sin\alpha\cos\beta & \sin\beta & \cos\alpha\cos\beta \end{pmatrix}, \tag{2.2}$$

where α and β are the corresponding Euler angles that define the drop orientation.

Projection of $\boldsymbol{u}_\infty$ into $\boldsymbol{x}$ results in a superposition of flows, which are categorised with respect to the arrangement of the velocity gradient relative to the internal interface. Flows with a velocity gradient normal and parallel to the internal interface are denoted by $\boldsymbol{v}$ and $\boldsymbol{w}$, respectively. Note that the use of the transformation matrix formulation shows the relevance of the drop orientation with regard to its resistance to the external flow; however, the appearance of the Euler angles in the resulting flows somewhat hinders their presentation. In order to circumvent this, the transformation is carried out equivalently in terms of fundamental operations (expressions are written in non-dimensional form):

$$\boldsymbol{v}_\perp = \boldsymbol{I}\cdot\boldsymbol{u}_\infty = x\boldsymbol{e}_z, \tag{2.3a}$$

$$\boldsymbol{v}_\parallel = -\tfrac{1}{2}\boldsymbol{E}^\infty\cdot\boldsymbol{x} + \tfrac{1}{2}\boldsymbol{e}_z\times\boldsymbol{x} = -z\boldsymbol{e}_x, \tag{2.3b}$$

$$\boldsymbol{v}^{xz} = -\boldsymbol{P}\cdot\boldsymbol{u}_\infty\cdot\boldsymbol{P} = x\boldsymbol{e}_x - z\boldsymbol{e}_z, \tag{2.3c}$$

$$\boldsymbol{w} = \boldsymbol{u}_\infty\times\boldsymbol{e}_x = \ x\boldsymbol{e}_y, \tag{2.3d}$$

where $\boldsymbol{I}$ is the identity tensor, the unit dyad $\boldsymbol{P} = -\boldsymbol{e}_k\boldsymbol{e}_l$, and the subscripts $\perp$ and $\parallel$ emphasise that the principal direction of the shear flow is normal and parallel to the internal interface, respectively. Note that $\boldsymbol{v}_\parallel$ simply results from a reflection of the straining part of the flow, that $\boldsymbol{v}^{xz}$ is a permutation of $\boldsymbol{u}_\infty$ into a hyperbolic flow, and that $\boldsymbol{w}$ is obtained via arrangement of the whole velocity field into a plane parallel to the internal interface. An illustration of the relation between the flows orthogonal to the internal interface is provided in figure 2 for further clarification. Arrangement of the straining axis of $\boldsymbol{v}^{xz}$ at a diagonal with the internal interface plus a rotational field yields either $\boldsymbol{v}_\parallel$ or $\boldsymbol{v}_\perp$, depending on the direction of the arrangement, as depicted in figure 2(*a*) and (*b*), respectively.

3. Governing equations

As a first step in exploring the behaviour of a Janus drop in a simple shear flow, fluid motion is analysed in the absence of inertia and in the limit of non-deformable interfaces. In terms of dimensionless groups, fluid motion is characterised by both a negligible Reynolds number, $Re = a^2G/\tilde{\nu}_0 \ll 1$, and capillary number, $Ca = a\,\tilde{\eta}_0\,G/\tilde{\sigma} \ll 1$, where a is the radius of the Janus drop, $\tilde{\nu}_0$ and $\tilde{\eta}_0$ are the kinematic and dynamic viscosity of the ambient, respectively, and $\tilde{\sigma}$ is the interfacial tension of the internal fluids (the limiting interfacial tension in practice, for instance see Torza & Mason 1970).

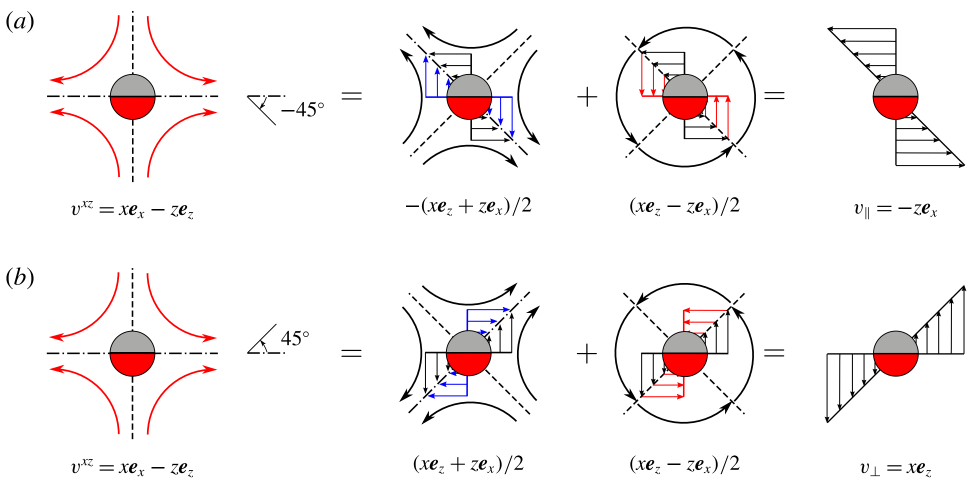

FIGURE 2. Transformation of $\boldsymbol{v}^{xz}$ into $\boldsymbol{v}_\parallel$ and $\boldsymbol{v}_\perp$. (*a*) Alignment of the straining axis (dot-dashed line) of $\boldsymbol{v}^{xz}$ at a -45° angle from its horizontal arrangement, plus a rotational field yields $\boldsymbol{v}_\parallel$. (*b*) Alignment of the straining axis at a 45° angle from its horizontal position, plus a rotational field results in $\boldsymbol{v}_\perp$.

The governing equations are written in non-dimensionalised form by adopting the following scales for length, fluid velocity and pressure: a, aG and $\tilde{\eta}_0 G$, respectively. Under the aforementioned assumptions, fluid flow is described by the Stokes equations, which are conveniently presented in spherical coordinates (r, ϑ, ϕ):

$$\nabla \boldsymbol{\cdot} \boldsymbol{u}^{(j)} = 0, \quad -\nabla p^{(j)} + \eta_j \nabla^2 \boldsymbol{u}^{(j)} = 0, \tag{3.1a}$$

$$\boldsymbol{n} \boldsymbol{\cdot} \boldsymbol{u}^{(j)} = 0, \quad [\boldsymbol{u}] = [\boldsymbol{n} \boldsymbol{\cdot} \boldsymbol{S}] = \boldsymbol{0}, \ \text{at } r = 1, \tag{3.1b}$$

$$\boldsymbol{n} \boldsymbol{\cdot} \boldsymbol{u}^{(1,2)} = 0, \quad [\boldsymbol{u}] = [\boldsymbol{n} \boldsymbol{\cdot} \boldsymbol{S}] = \boldsymbol{0}, \ \text{at } \vartheta = \pi/2, \tag{3.1c}$$

$$\boldsymbol{u}^{(0)} = \boldsymbol{u}_\infty \quad \text{as } r \to \infty, \tag{3.1d}$$

where $\boldsymbol{n}$ is the unit normal vector at interfaces, which is directed outward at every point on the outer surface and, analogously, at the internal interface it points from fluid '2' to fluid '1'. The fields $\boldsymbol{u}^{(j)}$ and $p^{(j)}$ denote the respective velocity and pressure of the jth fluid phase of viscosity $\eta_j = \tilde{\eta}_j/\tilde{\eta}_0$. All fluids are incompressible and Newtonian, $S^{(j)}_{lk} = -p^{(j)}\delta_{lk} + \eta_j(\nabla_l u^{(j)}_k + \nabla_k u^{(j)}_l)$, where δ_{lk} is the Kronecker delta. At interfaces $u_n = 0$ because fluids are immiscible. The brackets specify a jump of the fluid velocity and stresses at interfaces. At $r = 1$ this jump is directed from the internal to the ambient fluid, and at $\vartheta = \pi/2$ it is directed from fluid '2' to fluid '1'. Far away from the drop, the flow reduces to the undisturbed velocity $\boldsymbol{u}_\infty$ (any of the flows presented in § 2).

Continuity of the normal stress at interfaces only enters at the leading order of the expansion in the $Ca \ll 1$ limit. One may venture on determining shape distortions via a perturbation technique; however, it is expected that it will only bring a correction of $O(Ca)$ to the fluid forces. Accounting for shape distortions is most rewarding in studies concerned with the conditions for drop breakup, coalescence and rheology of a suspension (Stone & Leal 1990).

The force $\boldsymbol{F}$ on the drop is obtained by integrating the stresses at its surface ($r=1$):

$$\boldsymbol{F} = \oint \boldsymbol{n} \cdot \boldsymbol{S}\,\mathrm{d}A, \tag{3.2}$$

where A is the area of the outer surface, and the couple (or torque) $\boldsymbol{T}$ is calculated by:

$$\boldsymbol{T} = \oint \boldsymbol{x} \times (\boldsymbol{n} \cdot \boldsymbol{S})\mathrm{d}A. \tag{3.3}$$

The following scales render non-dimensional $\boldsymbol{F}$ and $\boldsymbol{T}$: $a^2\tilde{\eta}_0 G/2$ and $a^3\tilde{\eta}_0 G/2$, respectively, which guarantee that $\boldsymbol{T}$ reduces to that of a solid sphere when $\eta_1 = \eta_2 \gg 1$. Variation of $\boldsymbol{F}$ and $\boldsymbol{T}$ with the viscosity of the fluids is presented in terms of the drop mean viscosity $\eta = (\eta_2 + \eta_1)/2$ and viscosity contrast $\Delta\eta/2\eta = (\eta_2 - \eta_1)/(\eta_2 + \eta_1)$.

The viscosity contrast quantifies the deviation of the Janus drop from one with equal viscosities ($\eta_1 = \eta_2$). The limit of $\Delta\eta/2\eta \ll 1$ may be of particular interest to experimenters because of the similar viscosities of the constituent fluids in practice (Torza & Mason 1970; Nisisako *et al.* 2006). Nonetheless, the full range (0, 1) is considered for completeness. (Outside that domain there are no physical solutions.) In the limit of $\Delta\eta/2\eta \to 1$ and $\eta \gg 1$ the Janus drop is composed of a fluid of negligible and another of very high viscosity; however, this limit may not be of much use in practical settings.

4. Solution

Shear flow past a body is, inherently, a three-dimensional (3D) problem. For example, the disturbances caused by a fixed solid sphere result in a 3D flow. For a Janus drop subject to a simple shear flow, the motion of the fluid phases can be described via Lamb's generalised solution (Kim & Karrila 2005) (in non-dimensionalised form):

$$\boldsymbol{u}^{(j)} = \sum_{n=-\infty}^{\infty} \left[\frac{(n+3)\, r^2\, \nabla p_n^{(j)}}{2(n+1)(2n+3)} - \frac{n\, \boldsymbol{x}\, p_n^{(j)}}{(n+1)(2n+3)} \right] + \sum_{n=-\infty}^{\infty} \left[\nabla \Phi_n^{(j)} + r \nabla \chi_n^{(j)} \times \boldsymbol{e}_r \right], \tag{4.1}$$

where the following spherical harmonics characterise the flow of the suspending fluid:

$$p_n^{(0)} = \frac{2(-2n+1)}{(n+1)} E_n P_n^{(1)}(\theta) r^{-n-1} \cos\phi, \tag{4.2a}$$

$$\Phi_n^{(0)} = -\frac{E_n}{(n+1)} P_n^{(1)}(\theta) r^{-n-1} \cos\phi, \tag{4.2b}$$

$$\chi_n^{(0)} = -H_n P_n^{(1)}(\theta) r^{-n-1} \sin\phi, \tag{4.2c}$$

with corresponding series coefficients E_n, H_n, and $P_n^{(1)}(\theta)$ is the first associated Legendre polynomial of order n with $\theta = \cos\vartheta$. Analogously the internal flows are described by:

$$p_n^{(1,2)} = -\left\{ \frac{2(4n+1)}{(2n-1)} B_n^{(1,2)} \frac{P_{2n-1}^{(1)}(\theta)}{P_{2n-1}^{(1)}(0)} + \eta_{2,1} \frac{2(2n+1)(4n+3)}{(2n+3)} D_n \frac{P_{2n}^{(1)}(\theta)}{Q_{2n}(0)} r \right\} r^{2n-1} \cos\phi, \tag{4.3a}$$

$$\Phi_n^{(1,2)} = -\left\{\frac{B_n^{(1,2)}}{(2n+1)}\frac{P_{2n+1}^{(1)}(\theta)}{P_{2n+1}^{(1)}(0)} + \eta_{2,1}D_n\frac{P_{2n+2}^{(1)}(\theta)}{Q_{2n+2}(0)}r\right\} r^{2n+1}\cos\phi$$
$$+\left\{F_nP_{2n-1}^{(1)}(\theta) - \eta_{2,1}\,G_n\frac{P_{2n}^{(1)}(\theta)}{Q_{2n}(0)}r\right\} r^{2n-1}\cos\phi, \tag{4.3b}$$

$$\chi_n^{(1,2)} = \left\{A_n^{(1,2)}P_{2n}^{(1)}(\theta)r^{2n} - \eta_{2,1}G_n\frac{P_{2n-1}^{(1)}(\theta)}{P'_{2n-1}(0)}r^{2n-1}\right\}\sin\phi, \tag{4.3c}$$

with series coefficients $B_n^{(1,2)}$, $A_n^{(1,2)}$, D_n, F_n, G_n, and $Q_{2n}(0) = -2n(2n+1)P_{2n}(0)$. The tangent no-slip condition at the internal interface imposes the following constraint:

$$B_n^{(2)} - B_n^{(1)} = \frac{2n(2n-1)(2n+1)}{2(4n+1)}Q_{2n}(0)\,(A_n^{(2)} - A_n^{(1)}). \tag{4.4}$$

Although the obtained solution is exact, the series coefficients require numerical determination. Truncation of the expansion up to order $2N$ and matching of the velocity fields at the surface of the drop ($r=1$) results in a $(10N \times 10N)$ system of linear equations for the unknown coefficients, which is solved with the linear algebra package (lapack). The truncation order is increased systematically until convergence is achieved.

4.1. *Shear flow with a velocity gradient parallel to the internal interface*

It is straightforward to show that $\boldsymbol{w} = x\boldsymbol{e}_y$ results in $\boldsymbol{F} = \boldsymbol{T} = \boldsymbol{0}$, which is realised by noting that the Janus drop behaves as a single-phase drop. The particular, yet instructive, situation of a Janus drop with $\eta_1 = \eta_2$ reveals that the flows of a single-phase drop (Taylor 1932) satisfy the boundary value problem, and consequently, the forces and couples are identically zero. The situation is not so different for a Janus drop with different internal viscosities. As in the former case, the internal interface creates a system of velocity gradients that preserves the symmetric character of the flow, which guarantees that $\boldsymbol{F} = \boldsymbol{T} = \boldsymbol{0}$. It is expected that this result holds for a Janus drop with volume ratios of the internal fluids other than 1:1, despite the fact that the internal flows will differ from that of a single-phase drop. All fluids simply undergo a solid-body rotation and the straining field cannot impose a net force or torque in this configuration.

4.2. *Plane hyperbolic flow with a velocity gradient normal to the internal interface*

The force and couple imposed by the hyperbolic flow, $\boldsymbol{v}^{xz} = x\boldsymbol{e}_x - z\boldsymbol{e}_z$, on the Janus drop are considered. An illustration of the flow about the Janus drop is shown in figure 2(a).

Results show that $\boldsymbol{F} = \boldsymbol{T} = \boldsymbol{0}$ for a Janus drop with $\eta_1 = \eta_2$. Even then, $F_x = 0$ and $\boldsymbol{T} = \boldsymbol{0}$ for a Janus drop with different viscosities due to the symmetry of the flow. Thus, the underlying finding is that this flow-to-drop arrangement is an equilibrium one. Only the axisymmetric part of the flow imposes a force F_z that grows monotonically with $\Delta\eta/2\eta$, as shown by figure 3(a). Initially, the force is of $O(\Delta\eta/2\eta)$, which is best shown by the plot with $\eta = 1$, where deviation from linearity is less than 10 % up to $\Delta\eta/2\eta = 0.55$. At greater values of $\Delta\eta/2\eta$ the force grows quadratically because of a higher-order system of velocity gradients. In the dual limit of $\Delta\eta/2\eta \to 1$ and $\eta \gg 1$

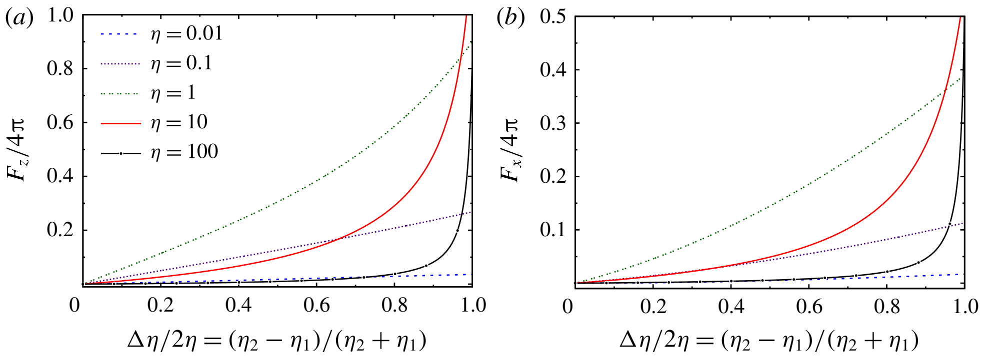

FIGURE 3. Variation of the force F_z (in units of $a^2\tilde{\eta}_0 G$) with the viscosity contrast at constant values of η when the Janus drop is subject to $\boldsymbol{v}^{xz}$ (*a*). The force F_x (in units of $a^2\tilde{\eta}_0 G$) on the Janus drop under the action of $\boldsymbol{v}_\parallel$ with increasing viscosity contrast at constant values of η (*b*).

the force F_z scales as $\eta_2/\eta_1 \gg 1$. It is worth noting that the force also diverges for a fixed 'slip–stick' sphere in the extreme limit of a perfect 'slip' surface (Ramachandran & Khair 2009). The plots clearly depict the non-monotonic dependence of the force F_z with the mean viscosity η. It is interesting to note that the net force reported here is the manifestation of the centre of hydrodynamic reaction $\boldsymbol{x}_{cr}$ being displaced from the flow stagnation point. In fact, it is found that the Janus drop experiences a zero net force when $\boldsymbol{x}_{cr}$ coincides with the flow stagnation point of a general straining flow (verified by independent calculations).

4.3. *Shear flows with a velocity gradient normal to the internal interface*

The forces and couples exerted by the shear flows, $\boldsymbol{v}_\parallel = -z\boldsymbol{e}_x$ and $\boldsymbol{v}_\perp = x\boldsymbol{e}_z$, are considered here. In view of the innate symmetry of the shear flows, it is evident that $\boldsymbol{F} = \boldsymbol{0}$ when $\eta_1 = \eta_2$. In particular, for $\boldsymbol{v}_\perp$ the force is always zero ($\boldsymbol{F} = \boldsymbol{0}$) regardless of $\Delta\eta/2\eta$; there can be no net force in the z direction, and also because the x component of the straining and rotating fields of $\boldsymbol{v}_\perp$ are equal in magnitude but opposite in direction, as shown in figure 2(*b*). Figure 3(*b*) depicts the effect of $\Delta\eta/2\eta$ on the force F_x when the Janus drop is subject to $\boldsymbol{v}_\parallel$, and it is notable that the effect is analogous to that found in a hyperbolic flow (figure 3*a*). It is important to point out that the appearance of a force is just the manifestation of $\boldsymbol{x}_{cr}$ being displaced from the centreline of the shear flow (in the coincident situation $\boldsymbol{F} = \boldsymbol{0}$ because of the zero coupling and shear-force tensors).

Figure 4 shows the variation of the resultant couple T_y (in units of $a^3\tilde{\eta}_0 G$) with the mean viscosity ($\eta = \eta_1 = \eta_2$). The solid line depicts T_y due to $\boldsymbol{v}_\perp$, and the dashed line shows its counterpart for $\boldsymbol{v}_\parallel$. It is readily seen that the couple in $\boldsymbol{v}_\perp$ is of greater magnitude than $\boldsymbol{v}_\parallel$, except in the extreme cases $\eta \ll 1$ (negligible viscous stresses) and $\eta \gg 1$ (solid-like), where the Janus drop behaves as an isotropic body and the direction of the shear flow becomes irrelevant. Figure 5 illustrates the velocity fields for both shear flows, and suggests that the couple is greater for $\boldsymbol{v}_\perp$ (figure 5*b*) because the internal interface prohibits, to a greater extent, the circulation flows of a single-phase drop. One may deduce from figure 4 that the resultant couple unfolds from both the straining and rotating components of the flow (otherwise, $\boldsymbol{v}_\parallel$ and $\boldsymbol{v}_\perp$ would generate

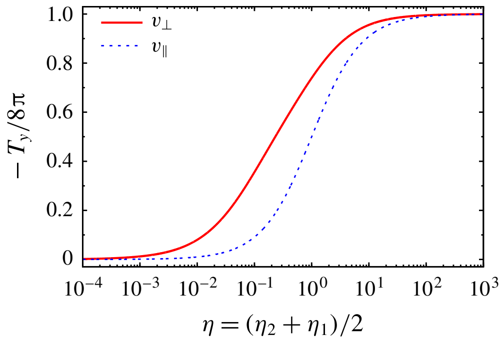

FIGURE 4. The couple T_y (in units of $a^3\tilde{\eta}_0 G$) on a Janus drop with $\eta_1=\eta_2$.

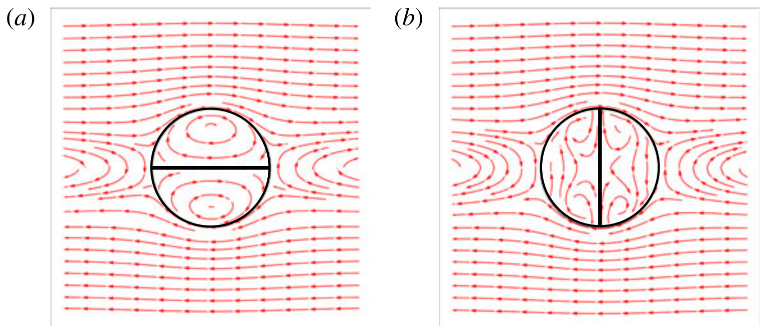

FIGURE 5. The velocity fields in and about a Janus drop subject to $\boldsymbol{v}_\parallel$ (*a*) and $\boldsymbol{v}_\perp$ (*b*).

the same curve). Perhaps, it is more relevant to point out that even a Janus drop with $\eta_1=\eta_2$ displays anisotropic properties, solely because of the presence of the internal interface.

The influence of $\Delta\eta/2\eta$ on T_y in $\boldsymbol{v}_\parallel$ and $\boldsymbol{v}_\perp$ is seen in figure 6 for selected values of the mean viscosity. It is noteworthy that the dependence of T_y on $\Delta\eta/2\eta$ is analogous to the dependence of the force in a streaming flow (Shklyaev *et al.* 2013), in the sense that the qualitative features are retained. (For small $\Delta\eta/2\eta$ the couple is $O(1)$, constant, and equal to the $\eta_1=\eta_2$ case.) Further increase of $\Delta\eta/2\eta$ induces a decay of T_y at a quadratic rate of the order of $(\Delta\eta/2\eta)^2$. This marked decrease of T_y is in agreement with the observation that the less viscous fluid sets up the magnitude of the couple.

4.4. *Cross-stream velocity of a Janus drop in a streaming flow*

A closed-form expression for the cross-stream velocity of a Janus drop is obtainable when the drop moves with a relative velocity $(u_z-u_{z,\infty})$ along the streamlines of a uniform flow. The external force required to sustain drop motion must pass through the centre of reaction $\boldsymbol{x}_{cr}$ to prevent rotation. The sought result is obtained by finding the migration velocity $u_{x,m}$ that cancels out the forces lateral to the undisturbed flow (this is analogous to the settling of anisotropic bodies presented by Happel & Brenner 1965). It is found that $u_{x,m}$ depends on the angle α from the scalar product $\boldsymbol{l}\cdot\boldsymbol{u}_\infty$, the

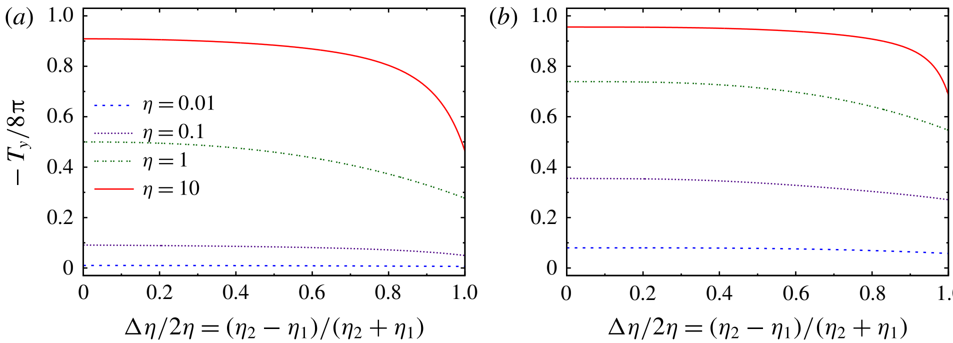

FIGURE 6. Variation of the couple T_y (in units of $a^3\tilde{\eta}_0 G$) with the viscosity contrast at constant values of the mean viscosity for $\boldsymbol{v}_\parallel$ (a) and $\boldsymbol{v}_\perp$ (b).

resistance functions to translation, X^A and Y^A (tabulated in the appendix), and the drop relative velocity:

$$u_{x,m} = \frac{\left(X^A - Y^A\right)\cos\alpha\sin\alpha}{X^A - \left(X^A - Y^A\right)\cos^2\alpha}\left(u_z - u_{z,\infty}\right). \tag{4.5}$$

Note that $u_{x,m}$ does not depend on the drop size due to its spherical shape. For example, a Janus drop with $\eta = 0.1$ exhibits a maximum ratio $u_{x,m}/(u_z - u_{z,\infty})$ of about 0.06.

5. Conclusions

The response (forces and couples) of a Janus drop under the shearing motion of the suspending fluid is investigated in the limit of negligible Reynolds number and capillary number (non-deformable interfaces). It is found that for an arbitrary drop orientation the shear flow can be broken down into flows with velocity gradients parallel and normal to the internal interface, which greatly reduces the analysis to four elemental problems. Although an exact solution is found via Lamb's generalised solution, numerical evaluation of the series coefficients is needed to calculate the force and couple on the Janus drop.

Only when the velocity gradient of the shear flow is parallel to the internal interface does the Janus drop behave as a single-phase drop. For transversal shear flows the no-penetration condition at the internal interface prohibits the circulation flows of a single-phase drop, and therefore novel phenomena is found. The resultant couple on the Janus drop arises from both the straining and rotating motions of the external flow, in analogy with a spheroid of revolution. In this case the Janus drop exhibits an anisotropic resistance to the shear flow because of the variation of the couple with the drop orientation.

The resistance matrix formulation reveals that at the centre of hydrodynamic reaction, $\boldsymbol{x}_{cr}$, the coupling tensor is identically zero, and the shear force vanishes. From these findings one can conclude that the equations that describe the position and orientation of a Janus drop 'freely' suspended in a shear flow are identical to those of a spheroid of revolution with Bretherton (1962) constant, $B = Y^H/Y^C$, with

https://doi.org/10.1017/jfm.2015.148 Published online by Cambridge University Press

tabulated values in the appendix. To avoid reproduction, these equations are omitted in this study but can be found elsewhere (Jeffery 1922; Kim & Karrila 2005). In contrast with other bodies of revolution with broken fore and aft symmetry, such as the spherical cap (Dorrepaal 1978) and an aggregate of spheres (Nir & Acrivos 1973), the results of this study reveal no tendency of a 'freely' suspended Janus drop to experience an axial 'drift' velocity in a shear flow. The drop matches the local streaming velocity, and its orientation follows the periodic orbit of an oblate spheroid.

It is interesting to note that a Janus drop with finite $\Delta\eta/2\eta$ can undergo a cross-flow migration in a shear flow by means of an external force (e.g. gravity) in the streamwise direction that lags the drop relative to the motion of the undisturbed flow. Due to the anisotropic resistance of the Janus drop to translation (see the appendix), part of the drag force acts lateral to the streamlines and induces cross-flow migration. The Janus drop does not rotate because of the coupling of the torque with translation (the external force must act at any point other than $\boldsymbol{x}_{cr}$). An exact expression (4.5) for the migration velocity of a Janus drop is found in a streaming flow and may be used as a rough estimate for the migration in a shear flow when $\Delta\eta/2\eta \ll 1$. The key observation is that lateral migration of a Janus drop can occur without the influence of walls and non-uniform velocity gradients, which are required to induce migration of a simple drop.

Acknowledgements

We are especially grateful to S. Shklyaev for his enlightening discussions, and to A. Khair for his instructive remarks. This publication is based on work supported by Award No. RUP1-7078-PE12 (joint grant with Ural Branch of the Russian Academy of Sciences) of the US Civilian & Development Foundation (CRDF Global) and by the National Science Foundation under Cooperative Agreement No. OISE-9531011. This work was partly supported by the National Science Foundation; CAREER Award (CBET-1055284).

Appendix A. The grand resistance matrix and Bretherton constant

The grand resistance matrix developed by Brenner (1963) for a body of arbitrary shape is presented for a Janus drop at its centre of hydrodynamic reaction $\boldsymbol{x}_{cr}$ in the limit of $\Delta\eta/2\eta \ll 1$. Note that, in practice, the internal viscosities are quite similar (Nisisako *et al.* 2006) and the effect of $\Delta\eta/2\eta$ on the non-zero resistances is of the order of $(\Delta\eta/2\eta)^2$.

The notation followed here for the resistance tensors is that of Kim & Karrila (2005):

$$\begin{pmatrix} \boldsymbol{F} \\ \boldsymbol{T} \\ \boldsymbol{S} \end{pmatrix} = \tilde{\eta}_0 \begin{pmatrix} \boldsymbol{A} & \tilde{\boldsymbol{B}} & \tilde{\boldsymbol{G}} \\ \boldsymbol{B} & \boldsymbol{C} & \tilde{\boldsymbol{H}} \\ \boldsymbol{G} & \boldsymbol{H} & \boldsymbol{M} \end{pmatrix} \begin{pmatrix} \boldsymbol{U}^\infty - \boldsymbol{U} \\ \boldsymbol{\Omega}^\infty - \boldsymbol{\omega} \\ \boldsymbol{E}^\infty \end{pmatrix}. \tag{A 1}$$

On account of the symmetry of the Janus drop the results are reported in terms of the resistance functions X, Y and Z associated with axisymmetric and transversal flows, respectively, relative to $\boldsymbol{x}_{cr}$, which is found to always be parallel to $\boldsymbol{l}$. Variation of the non-zero resistance functions with the mean viscosity η is presented in table 1.

η	$X^A/2\pi$	$Y^A/2\pi$	Y^C/π	$30\,Y^H/2\pi$	$3\,X^M/2\pi$	$3\,Y^M/2\pi$	B
0	2.000	2.000	0.000	0.000	4.000	8.000	0.0000
0.01	2.068	2.010	0.359	−0.701	4.059	8.085	−0.1302
0.1	2.339	2.091	1.786	−2.540	4.545	8.419	−0.0948
1.0	2.758	2.500	4.957	−2.436	7.000	9.225	−0.0328
2.0	2.852	2.667	5.997	−1.723	8.000	9.493	−0.0192
3.0	2.893	2.750	6.504	−1.331	8.500	9.623	−0.0136
4.0	2.917	2.800	6.806	−1.084	8.800	9.697	−0.0106
5.0	2.931	2.833	7.006	−0.913	9.000	9.750	−0.0087
10.0	2.963	2.909	7.460	−0.505	9.455	9.865	−0.0045
100.0	2.996	2.990	7.941	−0.056	9.941	9.985	−0.0005
∞	3.000	3.000	8.000	0.000	10.000	10.000	0.0000

TABLE 1. Variation of the non-zero scalar resistance functions and the Bretherton constant with the mean viscosity of the Janus drop (note that Z^M is identical to X^M).

References

BRENNER, H. 1963 The Stokes resistance of an arbitrary particle. *Chem. Engng Sci.* **18**, 1–25.

BRETHERTON, F. P. 1962 The motion of rigid particles in a shear flow at low Reynolds number. *J. Fluid Mech.* **14**, 284–304.

CHERVENIVANOVA, E. & ZAPRYANOV, Z. 1989 On the deformation of compound multiphase drops at low Reynolds numbers. *Physico-Chem. Hydrodyn.* **11**, 243–259.

DORREPAAL, J. M. 1978 The Stokes resistance of a spherical cap to translational and rotational motions in a linear shear flow. *J. Fluid Mech.* **84**, 265–279.

GUZOWSKI, J., KORCZYK, P. M., JAKIELA, S. & GARSTECKI, P. 2012 The structure and stability of multiple micro-droplets. *Soft Matt.* **8**, 7269–7278.

HAPPEL, J. & BRENNER, H. 1965 *Low Reynolds Number Hydrodynamics: with Special Applications to Particulate Media*. Prentice-Hall.

JEFFERY, G. B. 1922 The motion of ellipsoidal particles immersed in a viscous fluid. *Proc. R. Soc. Lond.* A **102**, 161–179.

JOHNSON, R. E. & SADHAL, S. S. 1985 Fluid mechanics of compound multiphase drops and bubbles. *Annu. Rev. Fluid Mech.* **17**, 289–320.

KIM, S. & KARRILA, S. J. 2005 *Microhydrodynamics Principles and Selected Applications*. Dover.

MANGA, M. & STONE, H. A. 1993 Buoyancy-driven interactions between two deformable viscous drops. *J. Fluid Mech.* **256**, 647–683.

MORTON, D. S., SUBRAMANIAN, R. S. & BALASUBRAMANIAM, R. 1990 The migration of a compound drop due to thermocapillarity. *Phys. Fluids* A **2**, 2119–2133.

NIR, A. & ACRIVOS, A. 1973 On the creeping motion of two arbitrary-sized touching spheres in a linear shear field. *J. Fluid Mech.* **59**, 209–223.

NISISAKO, T., TORII, T., TAKAHASHI, T. & TAKIZAWA, Y. 2006 Synthesis of monodisperse bicolored Janus particles with electrical anisotropy using a microfluidic co-flow system. *Adv. Mater.* **18**, 1152–1156.

RAMACHANDRAN, A. & KHAIR, A. S. 2009 The dynamics and rheology of a dilute suspension of hydrodynamically Janus spheres in a linear flow. *J. Fluid Mech.* **633**, 233–269.

ROSENFELD, L., LAVRENTEVA, O. M. & NIR, A. 2009 On the thermocapillary motion of partially engulfed compound drops. *J. Fluid Mech.* **626**, 263–289.

RUSHTON, E. & DAVIES, G. A. 1983 Settling of encapsulated droplets at low Reynolds numbers. *Int. J. Multiphase Flow* **9**, 337–342.

SADHAL, S. S. & OGUZ, H. N. 1985 Stokes flow past compound multiphase drops: the case of completely engulfed drops/bubbles. *J. Fluid Mech.* **160**, 511–529.

SHARDT, O., DERKSEN, J. J. & MITRA, S. K. 2014 Simulations of Janus droplets at equilibrium and in shear. *Phys. Fluids* **26**, 012104.

SHKLYAEV, S., IVANTSOV, A. O., DÍAZ-MALDONADO, M. & CÓRDOVA-FIGUEROA, U. M. 2013 Dynamics of a Janus drop in an external flow. *Phys. Fluids* **25**, 082105.

STONE, H. A. & LEAL, L. G. 1990 Breakup of concentric double emulsion droplets in linear flows. *J. Fluid Mech.* **211**, 123–156.

TAYLOR, G. I. 1932 The viscosity of a fluid containing small drops of another fluid. *Proc. R. Soc. Lond.* A **138**, 41–48.

TORZA, S. & MASON, S. G. 1970 Three-phase interactions in shear and electrical fields. *J. Colloid Interface Sci.* **33**, 67–83.

VUONG, S. T. & SADHAL, S. S. 1989 Growth and translation of a liquid–vapour compound drop in a second liquid. Part 1. Fluid mechanics. *J. Fluid Mech.* **209**, 617–637.